www.MaterialsViews.com

Monolayer Sheets

Rolling Up a Monolayer MoS_2 Sheet

Jianling Meng, Guole Wang, Xiaomin Li, Xiaobo Lu, Jing Zhang, Hua Yu, Wei Chen, Luojun Du, Mengzhou Liao, Jing Zhao, Peng Chen, Jianqi Zhu, Xuedong Bai, Dongxia Shi, and Guangyu Zhang**

Rolling up a thin solid film into nanoscale scrolls is an interesting topic in the field of nanoscience and nanotechnology. Clearly the geometry of a nanoscroll is different from its thin film matrix and would have a significant impact on its properties as well.[1–10] So far, various thin films of metals,[11] semiconductors[12,13] and insulators[14–16] have been explored for nanoscroll rolling-up. Recent advances in the discovery of a wide variety of 2D materials including graphene,[17–20] h-boron nitride (BN),[21] silicene,[22,23] and MoS_2,[24,25] just to mention a few, allow to explore the scrolling-up of them in an atomic-scale thickness limit. As predicted by theory, these nanoscrolls may have superior electronic and electromechanical properties[26–32] thus being useful in field effect transistors, tribology, catalysts, energy storage,[33–35] etc; however, the experimental realization of such nanoscrolls has only been achieved for graphene and BN.[36–43] Here, we report, for the first time, the rolling up a monolayer MoS_2 sheet. The nanoscrolls are formed from the edges or grain boundaries of MoS_2 sheet assisted by a weak argon plasma treatment. The plasma bombardment could selectively remove the top layer of sulfur atoms partially, causing a tensile stress within the MoS_2 basal plane and enabling the scroll formation. The structure of the as-fabricated MoS_2 nanoscrolls was systematically investigated by transmission electron microscope (TEM), atomic force microscopy (AFM), X-ray photoelectron spectroscopy (XPS), and Raman and photoluminescence (PL) spectra. The approach offers several advantages: (1) Convenient fabrication: the fabrication of MoS_2 nanoscrolls is fulfilled by Ar-plasma treatment and this approach is one step. (2) Solvents free: the Ar-plasma treatment is gas phase. (3) The high yielding of nanoscrolls: In our experiments, we used centimeter-scale continuous MoS_2 films on substrates as the raw material and the formation of nanoscrolls are everywhere across the entire substrate. (4) Scalable and compatible with standard plasma-etching techniques. Our approach provides a universal route toward rolling up 2D transition metal dichalcogenides into nanoscrolls for novel mechanical, electronic and optoelectronics applications.

In this study, monolayer MoS_2 samples are grown by chemical vapor deposition method as described in our previous report.[44] Typically such samples are fully covered on the substrate and polycrystalline with an average grain size of few hundreds nanometers. The AFM image of a typical sample grown on SiO_2 substrate is shown in **Figure 1**a. Our AFM images were taken by tapping mode AFM (MultiMode IIId, Veeco Instruments Inc.) at room temperature under ambient conditions. The scan rate is 1.33 Hz. Note that this sample is less than 100% coverage in order to see the substrate beneath. The as-grown MoS_2 continuous film was then treated argon plasma at a pressure of 0.3 Torr, plasma power of 25 W, and temperature of ≈150 °C for duration of 20 min. Since defect sites in this polycrystalline film are highly reactive; after plasma treatment, the separation of grain boundaries can be clearly seen, as shown in Figure 1b. Interestingly, the film starts to scroll along the separated edges when we further increase the plasma treatment duration to 40 min, as shown in Figure 1c. The height of these nanoscrolls varies from a few to tens of nm and a typical height ≈14.6 nm is shown in the Figure 1c. The height of these nanoscrolls varies from a few to tens of nm. A series of samples were treated under different Ar plasma powers to optimize the scrolling process (see Figure S1, Supporting Information). It was found that the optimum plasma power is 25 W; stronger plasma (e.g., 100 W) tends to cause too short nanoscrolls while it needs very long time to scroll in case of weaker plasma (e.g., 12 W) treatments. Noted that the scroll kinks rather than continuous straight scrolls in Figure S1b (Supporting Information), this is explained by the limited grain size of MoS_2. Scrolling occurs from the edges of these domains and kinks will be formed if the adjacent edges of one domain are not in parallel.

Besides, the nanoscroll length mainly depends on the grain size of the as-grown MoS_2. In Figure S1b (Supporting Information), the nanoscroll length is about 500 nm due to

Dr. J. L. Meng, G. L. Wang, X. M. Li, X. B. Lu, J. Zhang, H. Yu, Dr. W. Chen, L. J. Du, M. Z. Liao, Dr. J. Zhao, Dr. P. Chen, J. Q. Zhu, Prof. X. D. Bai, Prof. D. X. Shi, Prof. G. Y. Zhang
Beijing National Laboratory for Condensed Matter Physics and Institute of Physics
Chinese Academy of Science
Beijing 100190, China
E-mail: dxshi@aphy.iphy.ac.cn; gyzhang@aphy.iphy.ac.cn

Prof. G. Y. Zhang
Collaborative Innovation Center of Quantum Matter
Beijing 100190, China

Prof. G. Y. Zhang
Beijing Key Laboratory for Nanomaterials and Nanodevices
Beijing 100190, China

DOI: 10.1002/smll.201601413

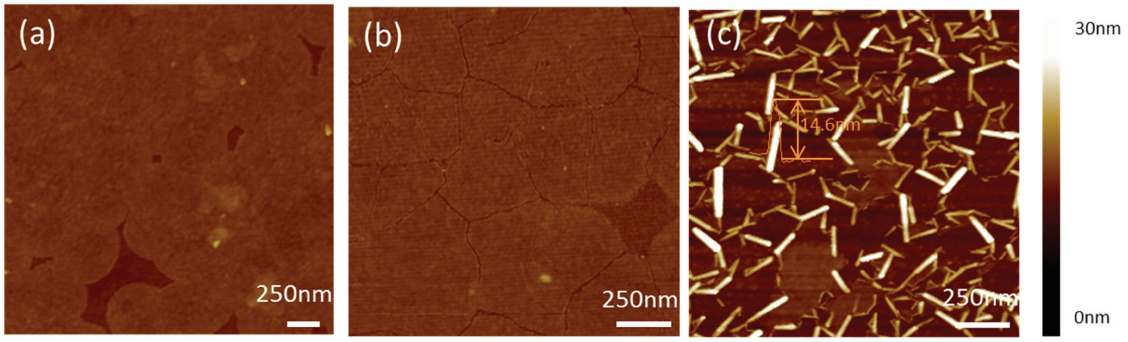

Figure 1. The forming process of MoS_2 nanoscroll. a) As-grown MoS_2 monolayer on SiO_2. b) Grain boundaries are separated. c) MoS_2 nanoscrolls formation along the separated boundaries.

the grain size of the MoS_2 is ≈500 nm. This is confirmed by the short length ≈70 nm nanoscroll formed by MoS_2 with grain size ≈70 nm treated by argon plasma (see Figure S2, Supporting Information).

Monolayer MoS_2 samples grown on various substrates, including sapphire, BN, and graphite substrates, were also investigated (Figure S3, Supporting Information), suggesting that the nanoscroll formation depends less on the substrates. It is noted that longer MoS_{2-x} nanoscrolls are formed on BN and graphite substrate, which suggests that MoS_2 film is easily scrolled on the weak bonding substrate.

Raman and PL spectra of the Ar plasma treated samples are shown in **Figure 2**. The spectra is carried out using a Horiba Jobin Yvon LabRAM HR-evolution Raman microscope(λ = 532 nm, power = 1 mW, beam spot size <1 μm). For as-grown MoS_2 monolayer samples, Raman peaks appear at ≈381 cm^{-1} (E_{2g}) and ≈401 cm^{-1} (A_{1g}) correspond to two characteristic in-plane and out-of-plane vibration modes (Figure 2a). The narrow frequency splitting Δ = ≈20 cm^{-1} between two modes is the fingerprint of MoS_2 monolayer. Note that a broadened peak appeared at ≈450 cm^{-1} comes from the double resonance of the longitudinal acoustic phonons.[45] For samples with separated grain boundaries, both A_{1g} and E_{2g} peaks become broader and weaker, indicating the existence of many disorders.[46] These disorders also induce the appearance of two additional peaks at ≈256 and 336 cm^{-1}. For scrolled samples, the blueshifted 256 cm^{-1} peak and the redshifted 336 cm^{-1} peak are resulted from the presence of a large amount of sulfur vacancies. PL characteristics of these samples are shown in Figure 2b. The as-grown MoS_2 has a shoulder peak at ≈608 cm^{-1}, known as B1 exciton, and a prominent peak at ≈660 cm^{-1}, known as A1 exciton. Surprisingly, once the sample is treated by Ar plasma, the PL peaks are quenched. This quenching phenomenon has also been observed previously and attributed to the sulfur removal in MoS_2 lattice,[47] which will be discussed in details in below.

In order to see the detailed structures of these MoS_2 nanoscrolls, we thus carried out high resolution transmission electron microscopy (HRTEM) studies. **Figure 3**a shows the HRTEM image of a typical sample transferred onto a TEM grid after nanoscroll formation. It can be clearly seen that this nanoscroll has a tubular structure with a hollow core of 5.573 nm and interlayer spacing of ≈0.4 nm (smaller than that of bulk MoS_2, ≈0.65 nm) which indicates the S atom removal. Beside, a sample shown in Figure S4 (Supporting Information) has one wall on one side and two walls on the other side, indicating a scroll structure. Interlayer spacing of this sample is even larger than ≈0.65 nm. Note that the tubular structure of nanoscrolls was confirmed by in situ rotating the sample during imaging (refer to an example shown in Figure S5, Supporting Information). In most cases, the selected electron diffraction patterns of the nanoscrolls

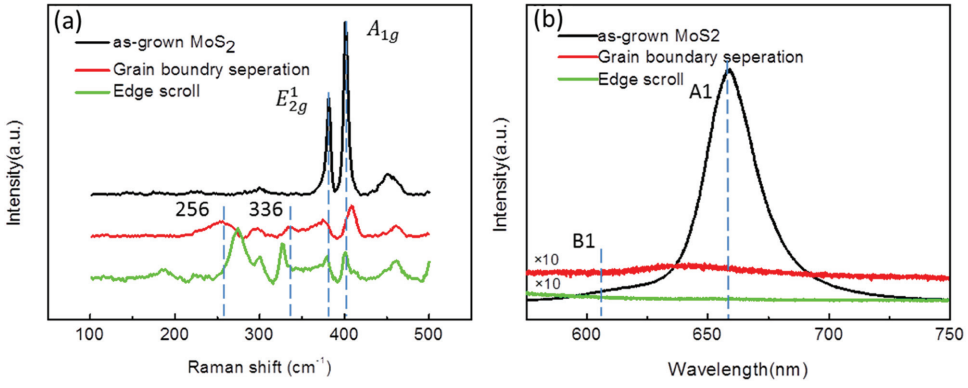

Figure 2. Raman and PL characteristics. a) Raman spectra of the as-grown MoS_2, MoS_2 with grain boundary separation and MoS_2 nanoscroll. b) PL spectra of the as-grown MoS_2, MoS_2 with grain boundary separation and MoS_2 nanoscroll.

www.MaterialsViews.com

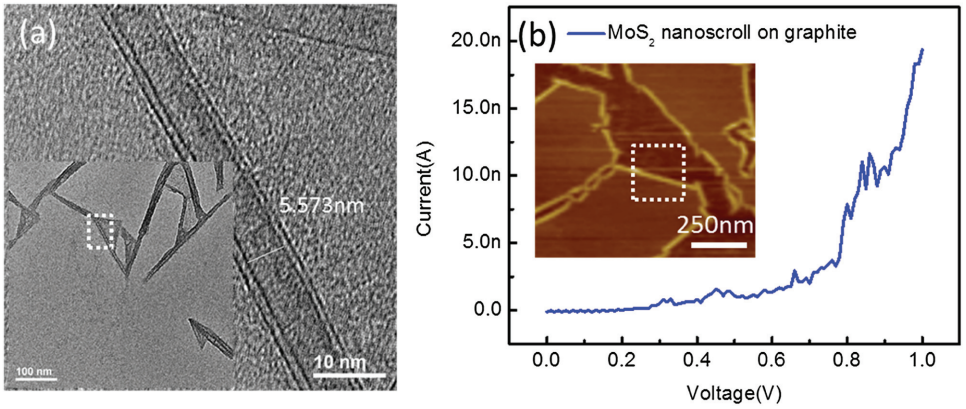

Figure 3. Structural and electrical properties of MoS_2 nanoscroll. a) TEM image of MoS_2 nanoscroll. (The inset is the low magnification TEM image and the marked area is zoomed-in.) b) Current–voltage curves of the graphite substrate and MoS_2 nanoscroll on the graphite substrate. The inset is the AFM image of MoS_2 nanoscroll on graphite substrate.

consist of multisets of hexagonal patterns, suggesting a random scrolling orientation.

For the local electrical measurement, we combined AFM with semiconductor analyzer Agilent B1500. A conductive AFM tip (Cr coated) acts as a local electrode and the sample holder as the other electrode. The two electrodes are connected to the Agilent B1500. We choose MoS_2 on graphite due to the metallic graphite. The graphite is connected to the holder by silver glue. The AFM tip is programmed to the nanoscroll by AFM nanoscripts lithography mode. Bias of the AFM tip was swept from 0 to 1 V while the graphite was connected to the ground from external Agilent B1500. The *I–V* curve is shown in Figure 3b. The current is ≈20 nA at a bias of 1 V. The nonlinear *I–V* curve suggests the existence of an energy barrier between graphite and semiconductor MoS_2.

XPS was further used to analyze the MoS_2 nanoscroll composition. The spectra are carried out using a Thermofisher-ESCALAB 250Xi microscope (AlKαX-ray). For a typical polycrystalline MoS_2 film samples after Ar plasma treatments, similar to those shown in Figure 1, the Mo-3d and S-2p core levels are all visible (**Figure 4**). All spectra were normalized to the C-1s binding energy of 284.7 eV. The Mo-$3d_{3/2}$ and $3d_{5/2}$ doublets are independent Gaussian peaks while S-$2p_{1/2}$ and $2p_{3/2}$ peaks show overlap. After Ar plasma treatment, the peaks for Mo doublets and S doublets all show a redshift by ≈1.1 eV, which is due to the pinning of fermi level at the top of the MoS_2 valence band induced by the defects states.[48–50] The extrapolated S/Mo atomic ratio is ≈2.0, ≈1.4, and ≈1.0 for the as-grown MoS_2, grain boundary separated MoS_2 and scrolled MoS_2, respectively. Note that these atomic ratios may not be accurate, since XPS is only a semiquantitative tool for elemental analysis. However, it is no doubt that, the obvious decreasing of S/Mo atomic ratio suggests the removal of sulfur atoms after Ar plasma treatments. Moreover, it is also reasonably assume that the removal occurs only on the surface (here, the top sulfur layer of the sandwiched MoS_2 atomic layer) which is exposed to the Ar plasma. In later discussions, we will see, this assumption is essential for us to understand the rolling-up mechanism.

The schematic diagram of the process of MoS_2 is shown in **Figure 5**. As we all know, Ar plasma bombardment is a physical process rather than a chemical reaction. It can destroy the MoS_2 lattice by kicking the very top sulfur atoms out when the kinetic energy of Ar ions is larger than the Mo–S

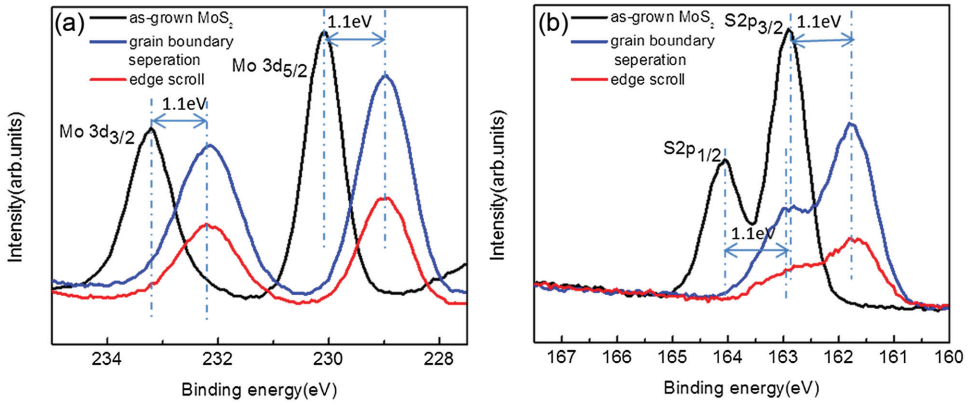

Figure 4. The XPS analyses of Mo and S element. a) The XPS spectra of Mo atom core level of as-grown MoS_2, MoS_2 with grain boundary separation and MoS_2 nanoscroll. The corresponding S/Mo ratio is 1.96, 1.04, and 1.02. b) The XPS spectra of S atom core level of as-grown MoS_2, MoS_2 with grain boundary separation and MoS_2 nanoscroll.

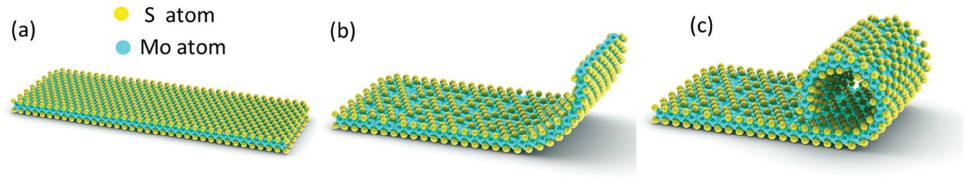

Figure 5. The schematic diagram of the process of MoS_2 nanoscroll formation. a) As-grown MoS_2 monolayer. b) The rolling up of MoS_2 along its edges. c) MoS_2 nanoscrolls formation.

binding energy. As-created dangling bonds could not be saturated in the inert gas of Ar, causing an out-of-plane strain. It has been modeled by Han et al. that a single sulfur vacancy line in MoS_2 can induce larger strain near the vacancy line with ≈4.6% tensile formation on one side and –2.5% compressive formations on the other side, leading to a severe out-of-plane distortion as high as 42.8°.[51] This strain-induced large out-of-plane distortion can thus trigger the rolling-up of a single layer of MoS_2 from its edges. Removing the S atom from top layer is necessary for scroll formation. During the scrolling process, the already formed scrolls are also exposed to the argon plasma. These exposed S atom, though not all of them, would be further removed and drive the scrolling process through covalent bond formation.

As discussed above, the dangling bond formation is a key factor for the rolling-up process. In order to verify this point of view, we also carried out a series of control experiments. First, hydrogen, nitrogen, oxygen, and mixture gases of Ar/H_2 or Ar/O_2 plasma treatments were applied to our MoS_2 samples, but rolling-up of MoS_2 was observed in none of these cases, see Figure S6 (Supporting Information). The failure can be explained by the fact that these gas atoms except argon can passivate, or saturate the formed dangling bonds formed in, the MoS_2 at the edges or sulfur vacancies. See supporting Information for further analysis. Second, we also found that this Ar-plasma treatment induced rolling-up of MoS_2 is also applicable for other 2D transition metal dichalcogenides (TMDCs) such as WS_{2-x} and WSe_{2-x} (see Figure S9, Supporting Information).

These MoSx($1 < x < 2$) nanoscrolls are potentially useful for catalysis as the sulfur-deficient area are defective and could act as a reaction center for catalytic reaction.

In summary, a unique fabrication approach for rolling MoS_2 up into nanoscrolls is reported. It is concluded that the generation of S vacancies caused by argon plasma treatment is the key factor of scrolling. This convenient, solvents-free, and high-yielding approach for nanoscroll fabrication is also suitable for the fabrication of other 2D transition metal dichalcogenides.

Experimental Section

Preparation of TEM Sample: The continuous monolayer MoS_2 was first grown on the SiO_2 substrate. Then the monolayer MoS_2 on SiO_2 was treated by Ar plasma at a pressure of 0.3 Torr and plasma power of 25 W for duration of 40 min. The as-made MoS_2 nanoscroll was then spin-coated layer of PMMA(Poly(methyl methacrylate)) (950 5% in anisole) at 3000 rpm for 60 s and then baked at 180 °C and repeated the spin-coating and baking process again. The coated MoS_2 nanoscroll was wet etched by HF solution (HF: deionized water = 1:2). The PMMA/MoS_2 nanoscroll film was transferred onto the Cu grid. Then, the PMMA was dissolved by lift-off process in acetone for about 10 h. Finally, the transferred MoS_2 nanaoscroll/Cu grid was annealed at the atmosphere of Ar (100 sccm)/H_2 (10 sccm) at 450 °C.

Supporting Information

Supporting Information is available from the Wiley Online Library or from the author.

Acknowledgements

This work was supported by the National Basic Research Program of China (973 Program, Grant No. 2013CB934500), the National Science Foundation of China (NSFC, Grant Nos. 51572289, 61325021, and 91323304), and Strategic Priority Research Program (B) of the Chinese Academy of Sciences (Grant No. XDB07010100).

[1] D. Berman, S. A. Deshmukh, S. K. R. S. Sankaranarayanan, A. Erdemir, A. V. Sumant, *Science* **2015**, *348*, 1118.
[2] O. G. Schmidt, K. Eberl, *Nature* **2001**, *410*, 168.
[3] B. Koch, A. K. Meyer, L. Helbig, S. M. Harazim, A. Storch, S. Sanchez, O. G. Schmidt, *Nano Lett.* **2015**, *15*, 5530.
[4] X. Liu, J. Zhang, W. Si, L. Xi, B. Eichler, C. Yan, O. G. Schmidt, *ACS Nano* **2015**, *9*, 1198.
[5] I. Mönch, D. Makarov, R. Koseva, L. Baraban, D. Karnaushenko, C. Kaiser, K.-F. Arndt, O. G. Schmidt, *ACS Nano* **2011**, *5*, 7436.
[6] L. Soler, V. Magdanz, V. M. Fomin, S. Sanchez, O. G. Schmidt, *ACS Nano* **2013**, *7*, 9611.
[7] D. Grimm, C. C. Bof Bufon, C. Deneke, P. Atkinson, D. J. Thurmer, F. Schäffel, S. Gorantla, A. Bachmatiuk, O. G. Schmidt, *Nano Lett.* **2013**, *13*, 213.
[8] S. Schwaiger, M. Bröll, A. Krohn, A. Stemmann, C. Heyn, Y. Stark, D. Stickler, D. Heitmann, S. Mendach, *Phys. Rev. Lett.* **2009**, *102*, 163903.
[9] P. Froeter, Y. Huang, O. V. Cangellaris, W. Huang, E. W. Dent, M. U. Gillette, J. C. Williams, X. Li, *ACS Nano* **2014**, *8*, 11108.
[10] C. S. Martinez-Cisneros, S. Sanchez, W. Xi, O. G. Schmidt, *Nano Lett.* **2014**, *14*, 2219.
[11] P. Cendula, S. Kiravittaya, I. Mönch, J. Schumann, O. G. Schmidt, *Nano Lett.* **2011**, *11*, 236.
[12] I. S. Chun, A. Challa, B. Derickson, K. J. Hsia, X. Li, *Nano Lett.* **2010**, *10*, 3927.
[13] J. Zang, M. Huang, F. Liu, *Phys. Rev. Lett.* **2007**, *98*, 146102.
[14] R. Ma, Y. Bando, T. Sasaki, *J. Phys. Chem. B* **2004**, *108*, 2115.

[15] J. Li, J. Zhang, W. Gao, G. Huang, Z. Di, R. Liu, J. Wang, Y. Mei, *Adv. Mater.* **2013**, *25*, 3715.
[16] W. Huang, X. Yu, P. Froeter, R. Xu, P. Ferreira, X. Li, *Nano Lett.* **2012**, *12*, 6283.
[17] K. S. Novoselov, A. K. Geim, S. V. Morozov, D. Jiang, Y. Zhang, S. V. Dubonos, I. V. Grigorieva, A. A. Firsov, *Science* **2004**, *306*, 666.
[18] A. H. Castro Neto, F. Guinea, N. M. R. Peres, K. S. Novoselov, A. K. Geim, *Rev. Mod. Phys.* **2009**, *81*, 109.
[19] Y. Zhang, Y.-W. Tan, H. L. Stormer, P. Kim, *Nature* **2005**, *438*, 201.
[20] K. S. Novoselov, A. K. Geim, S. V. Morozov, D. Jiang, M. I. Katsnelson, I. V. Grigorieva, S. V. Dubonos, A. A. Firsov, *Nature* **2005**, *438*, 197.
[21] L. Song, L. Ci, H. Lu, P. B. Sorokin, C. Jin, J. Ni, A. G. Kvashnin, D. G. Kvashnin, J. Lou, B. I. Yakobson, P. M. Ajayan, *Nano Lett.* **2010**, *10*, 3209.
[22] P. Vogt, P. De Padova, C. Quaresima, J. Avila, E. Frantzeskakis, M. C. Asensio, A. Resta, B. Ealet, G. Le Lay, *Phys. Rev. Lett.* **2012**, *108*, 155501.
[23] A. Fleurence, R. Friedlein, T. Ozaki, H. Kawai, Y. Wang, Y. Yamada-Takamura, *Phys. Rev. Lett.* **2012**, *108*, 245501.
[24] K. F. Mak, C. Lee, J. Hone, J. Shan, T. F. Heinz, *Phys. Rev. Lett.* **2010**, *105*, 1368058.
[25] Y. Ma, L. Kou, X. Li, Y. Dai, S. C. Smith, T. Heine, *Phys. Rev. B* **2015**, *92*, 085427.
[26] S. F. Braga, V. R. Coluci, S. B. Legoas, R. Giro, D. S. Galvão, R. H. Baughman, *Nano Lett.* **2004**, *4*, 881.
[27] Y. Chen, J. Lu, Z. Gao, *J. Phys. Chem. C* **2007**, *111*, 1625.
[28] H. Pan, Y. Feng, J. Lin, *Phys. Rev. B* **2005**, *72*, 085415.
[29] J. S. Lauret, R. Arenal, F. Ducastelle, A. Loiseau, M. Cau, B. Attal-Tretout, E. Rosencher, L. Goux-Capes, *Phys. Rev. Lett.* **2005**, *94*, 037405.
[30] G. Y. Guo, J. C. Lin, *Phys. Rev. B* **2005**, *71*, 165402.
[31] J. Xiao, M. Long, X. Li, H. Xu, H. Huang, Y. Gao, *Sci. Rep.* **2014**, *4*, 4327.
[32] M. Ghorbani-Asl, N. Zibouche, M. Wahiduzzaman, A. F. Oliveira, A. Kuc, T. Heine, *Sci. Rep.* **2013**, *3*, 2961.
[33] G. Mpourmpakis, E. Tylianakis, G. E. Froudakis, *Nano Lett.* **2007**, *7*, 1893.
[34] M. Strojnik, A. Kovic, A. Mrzel, J. Buh, J. Strle, D. Mihailovic, *AIP Adv.* **2014**, *4*, 097114.
[35] D. Maharaj, B. Bhushan, *Mater. Lett.* **2015**, *142*, 207.
[36] H. Shioyama, T. Akita, *Carbon* **2003**, *41*, 179.
[37] L. M. Viculis, J. J. Mack, R. B. Kaner, *Science* **2003**, *299*, 1361.
[38] J. W. Liu, J. Xu, Y. Ni, F. J. Fan, C. L. Zhang, S. H. Yu, *ACS Nano* **2012**, *6*, 4500.
[39] X. Xie, L. Ju, X. Feng, Y. Sun, R. Zhou, K. Liu, S. Fan, Q. Li, K. Jiang, *Nano Lett.* **2009**, *9*, 2565.
[40] S. Anton, M. David, S. Gamini, P. J. Ouseph, C. S. Jayanthi, W. Shi-Yu, *Nanotechnology* **2009**, *20*, 055611.
[41] R. Bacon, *J. Appl. Phys.* **1960**, *31*, 283.
[42] I. D. Barcelos, L. G. Moura, R. G. Lacerda, A. Malachias, *Nano Lett.* **2014**, *14*, 3919.
[43] X. Chen, R. A. Boulos, J. F. Dobson, C. L. Raston, *Nanoscale* **2013**, *5*, 498.
[44] J. Zhang, H. Yu, W. Chen, X. Tian, D. Liu, M. Cheng, G. Xie, W. Yang, R. Yang, X. Bai, D. Shi, G. Zhang, *ACS Nano* **2014**, *8*, 6024.
[45] M. A. Pimenta, E. del Corro, B. R. Carvalho, C. Fantini, L. M. Malard, *Acc. Chem. Res.* **2015**, *48*, 41.
[46] N. T. Mcdevitt, J. S. Zabinski, M. S. Donley, J. E. Bultman, *Appl. Spectrosc.* **1994**, *48*, 733.
[47] Q. Ma, P. M. Odenthal, J. Mann, D. Le, C. S. Wang, Y. M. Zhu, T. Y. Chen, D. Z. Sun, K. Yamaguchi, T. Tran, M. Wurch, J. L. McKinley, J. Wyrick, K. Magnone, T. F. Heinz, T. S. Rahman, R. Kawakami, L. Bartels, *J. Phys.: Condens. Mater* **2013**, *25*, 252201.
[48] J. R. Lince, D. J. Carre, P. D. Fleischauer, *Langmuir* **1986**, *2*, 805.
[49] M. Donarelli, F. Bisti, F. Perrozzi, L. Ottaviano, *Chem. Phys. Lett.* **2013**, *588*, 198.
[50] C. B. Roxlo, H. W. Deckman, J. Gland, S. D. Cameron, R. R. Chianelli, *Science* **1987**, *235*, 1629.
[51] Y. Han, J. Zhou, J. Dong, *Appl. Surf. Sci.* **2015**, *346*, 470.

Received: April 25, 2016
Published online: June 20, 2016